Analysis of a gravity dam considering the application of passive reinforcement

E.M. Bretas
Universidade do Minho, Guimarães, Portugal

P. Léger
Ecole Polytechnique de Montréal, Montréal, Canada

J.V. Lemos
LNEC, Lisboa, Portugal

P.B. Lourenço
Universidade do Minho, Guimarães, Portugal

ABSTRACT: Small concrete gravity dams are sometimes built using passive steel anchors to enhance their stability for the applied loads. It is important to assess the amount of internal tensile and shear forces resisted by the anchors to verify their structural adequacy. This paper presents the application of the distinct element method to study the magnitude and distribution of internal anchor forces. Comprehensive parametric analyses considering the anchor shear stiffness and the friction angle of the dam-foundation interface have been performed on a small dam 3 m high. The case of several anchors along the section was also investigated. It is shown that (a) the required displacements to induce anchor loads are very small (of the order of $10x10^{-3}$ mm of crack opening), (b) that the anchor shear stiffness has small impact in the load share between anchor and concrete, and finally (c) that strength properties of rock-concrete interface play a key role in the structure behavior.

1 INTRODUCTION

Several existing small concrete gravity and buttress dams (less than approximately 7m high) have been constructed with passive steel reinforcement anchors to ensure adequate structural stability for usual, unusual, and extreme load combinations (Fig.1).

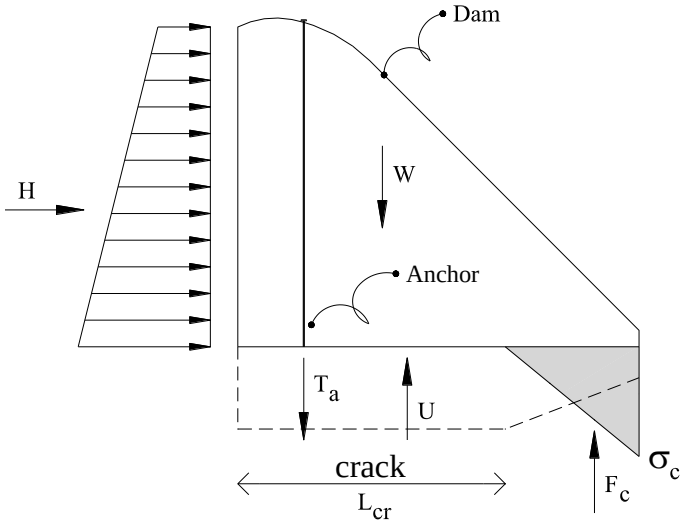

Figure 1. Gravity dam with passive anchor (H – Hydrostatic load, W – Weight, T_a – Tensile force, U – Uplift force, σ_c – Concrete stress, F_c – Concrete force, L_{cr} – Crack length)

It is also possible to consider adding passive reinforcement to existing small gravity dams that do not meet current stability criteria. The basic advantages of using passive reinforcement to a section subjected to axial (P) and shear loads (H) as well as bending moments (M) are (a) the increase in concrete compressive force resultant thus increasing the shear strength that can be mobilized, V_c, (b) a small decrease in crack length, $L_{cr,}$ as compared to unreinforced sections, and (c) the direct dowel action of the anchor, V_a, increasing the shear strength of the section (Fig.2).

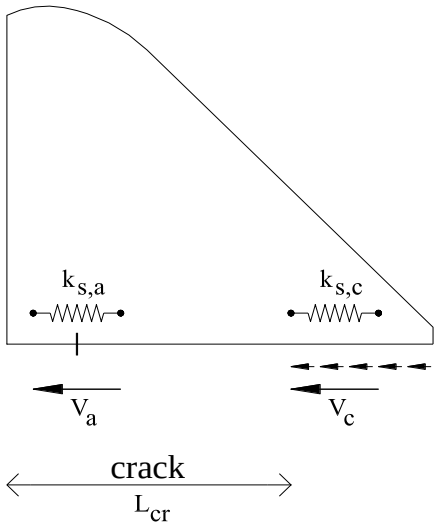

Figure 2. Shear forces and stiffnesses (H – Hydrostatic load, V_a – Anchor shear force, V_c – Concrete shear force, $k_{s,a}$ – Anchor shear stiffness, $k_{c,a}$ – Concrete shear stiffness, L_{cr} – Crack length)

However, the use of passive anchors presents also some disadvantages. A first objection is that a small amount of displacement is required to induce axial and shear forces in the anchors (USACE 2005). Durability, that is mainly deterioration due to corrosion, is of concern, fatigue has also been discussed however, the induced stress level are low as well as the stress variations due to water level fluctuation, seasonal temperature variations and ice loads for dams located in northern regions.

To assess the integrity of the anchor one needs to compute the tensile, T_a, and shear force, V_a, that will be induced by the applied loads including uplift pressures. Interaction formulas can then be applied:

$$\left(\frac{T_a}{T_{a,\max}}\right)^2+\left(\frac{V_a}{V_{a,\max}}\right)^2\le 1 \qquad (1)$$

The purpose of this paper is to present a computational procedure using the distinct element method (a) to assess the tensile force developed in the anchors, T_a, and how the applied total shear force H is split among the anchor, V_a, and the concrete, V_c, contributions. These forces represent the driving shear forces. Secondary failure mechanisms should be verified to ensure the integrity of the anchor (pull-out of a rock mass thus uplifting of the anchor, bond slip at the various interfaces, bearing failure (Wyllie 1999)), however, this is outside of scope of this paper. A sliding safety factor could be determined from the ratio of the maximum shear force that could be mobilized to the applied shear load. The paper is organized as follows. We first present formulations to compute the axial and shear stiffnesses as well as the maximum strength that could be developed in the anchors. The distinct element method, used to solve the equilibrium equation with a concrete-rock interface reinforced by passive anchors, is outlined.

An extensive parametric analysis is performed to assess the effects of the shear stiffness of the anchor and the friction angle of the concrete-rock interface on the distribution of the shear load at the rock-concrete interface. It is shown that (a) the required displacements to induce anchor loads are very small (of the order of $10\text{x}10^{-3}$ mm of crack opening), (b) that the anchor shear stiffness has small impact in the load share between anchor and concrete, and finally that strength properties of rock-concrete interface play a key role in the structure behavior.

2 MECHANICAL AND STRENGTH PROPERTIES OF PASSIVE ANCHORS

For gravity dams, to assess a sliding failure scenario on a discontinuity interface it is interesting to identify the contribution of passive anchors in the total shear strength. The action of a passive anchor, fully grouted, increases the compressive force developed in the interface. Dowel action and increased frictional forces are developed when a small relative displacement between the two sides of the discontinuity under consideration is taking place (Pells 1974, Haas 1976, Azuar et al. 1979).

To develop a model for anchor behavior, the shear stiffness of the passive anchor must to be determined. There are several possible approaches as, for example, one proposed by St. John and Van Dillen (1983), who considered the bar as a short beam,

$$K_{s,a}=\frac{3E_bI}{2L_d^3} \qquad (2)$$

where,

E_b – Young's modulus of the bar
I – moment of inertia of the bar
L_d – decay length of the bending stress in the bar

To take account with the grout effect, Lorig (1985) proposed the following equation

$$K_{s,a}=E_bI\beta^3 \qquad (3)$$

where,

$$\beta=\left(\frac{K}{4E_bI}\right)^{\frac{1}{4}} \qquad (4)$$

$$K=\frac{2E_g}{\left(\frac{d_1}{d_2}-1\right)} \qquad (5)$$

I – moment of inertia of the bar
E_g - Young's modulus of the grout
d_1 – reinforcement diameter
d_2 – hole diameter

The axial stiffness of the anchor could be first estimated as AE/L_d more complicated formulas have been presented in UDEC User's Manual (2004) and involves the grout shear modulus as well as the Young's modulus of the steel reinforcement

Based on the tests carried by Bjurstrom (1974), an empirical rule to estimate the maximum anchor shear resistance was developed,

$$V_{ult} = 0.67 d_1^2 \sqrt{\sigma_b \sigma_c} \quad (6)$$

where,

σ_b - uniaxial compressive strength of rock

σ_c - yield strength of bar

To provide an assessment of the safety condition of the dam in terms of shear failure, a global safety factor (SF) could be estimated, which compares the shear resistance and driving shear force, given by

$$SF = \frac{(V_c + V_a)}{H_{us} - H_{ds}} \quad (7)$$

where,

V_c – Concrete shear force
V_a – Anchor shear force
H_{us} – Upstream hydrostatic force
H_{ds} – Downstream hydrostatic force

To apply this formulation one needs to know V_a and, by corollary, V_c. Theoretically, for small (fairly rigid) gravity dams with passive anchors , the structure may be assumed as two springs in parallel, one represents the anchor shear stiffness $K_{s,a}$ and the other the concrete shear stiffness $K_{s,c}$. Thus V_a and V_c are determined by

$$V_a = \frac{H(K_{s,a})}{K_{s,a} + K_{s,c}} \quad (8)$$

$$V_c = \frac{H(K_{s,c})}{K_{s,a} + K_{s,c}} \quad (9)$$

where,

$$H = H_{us} - H_{ds} \quad (10)$$

Because the anchor behavior depends on the passive anchor slip in the plane of the discontinuity and the relative stiffness of the anchor and concrete it is of interest to address this problem using numerical tools that allow the explicit modeling of axial and shear displacement, such as those based on distinct element method.

3 DISTINCT ELEMENT METHOD FOR GRAVITY DAM ANALYSIS

The Distinct Element Method (DEM) was initially developed for analysis of geotechnical problems, particularly in the solution of models that have high discontinuity, with importance in the process of rupture. DEM allows explicit modeling of joints and use of appropriate constitutive models to them. This feature is mainly reflected in the ability of DEM to predict the mechanisms and loads displacement response up to failure.

The solution is based on time integration of the equation of motion (2nd Newton's Law) of each degree of freedom, using the method of central difference. Static and dynamic analyses are performed using the same calculation scheme. The static response is obtained by a dynamic relaxation process by means of applying a damping force sufficiently high to dissipate kinetic energy and reach the solution of static equilibrium.

The numerical application developed in this work, designated as DEC-DAM (Distinct Element Code for gravity DAM analysis), is an implementation of DEM to gravity dam analyses. Using deformable blocks, discretized by quadrilateral finite elements (four sides and four nodal points), with shape functions of 1st order, whose integration is done with four Gauss points. The contact between the blocks is of the type face-to-face and adopts a linear distribution of stress.

The constitutive model of joints is following a Mohr-Coulomb criterion, defined from the parameters of cohesion, friction angle, tensile strength and normal and shear stiffnesses that control elastic deformation of the joints. In general, the residual value of cohesion is zero, after exceeding the maximum value of shear stress (peak value), the shear strength becomes conditioned only by the friction angle. The concrete normal stress is limited by its tensile strength very often taken as zero at the dam-foundation interface. After joint opening, the contact could still remain active, and is able to model shear-keys or another interlock mechanism.

One of the features specific to the case of gravity dams is the need to include uplift pressure on a cracked surface. The interfaces under study are parameterized and is possible throughout the analysis obtain specific information, for example the crack length, beside if the crack still in progress, the uplift pressure can then be updated.

Another tool is the modeling of passive anchors between two blocks (local reinforcement). After installing an anchor, the applied forces (normal and

shear) in the blocks, depends on their relative displacement. The behavior of anchor is controlled by the axial and shear stiffnesses, axial and shear ultimate capacities and axial and shear failure strains.

Throughout the development of DEC-DAM, validation tests are carried out with 3DEC (2003) and UDEC numerical applications, both developed by Itasca. Similar procedure was followed in this study, whose results were confirmed by 3DEC (Bretas et al., 2010a and 2010b).

4 APPLICATION TO A SMALL EXISTING DAM

4.1 *System analyzed*

The structure under study is a small dam (Fig. 3) located in Canada, with an overflow profile, height 2.9m and base width of 3.65m, laid out in a wide valley in a straight line plan position, without vertical contraction joints or drainage system. The section is reinforced with a passive anchor (Fig. 4), 29.9mm diameter, positioned approximately 0.6m from the upstream heel.

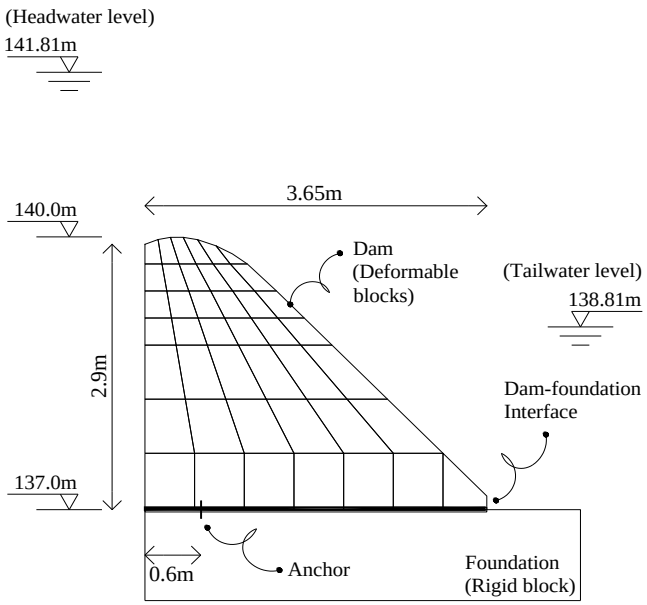

Figure 3. DEC-DAM model with geometry definition and load case

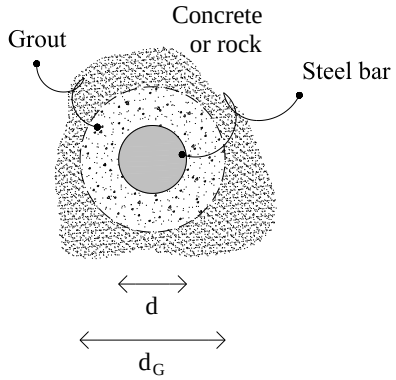

Figure 4. Anchor cross-section (30M Steel Bar) (d=29.9mm, σ_y=400MPa, A=700mm^2, E=200GPa, G=18GPa, d_G=64mm)

Analysis was made for a flood scenario, with headwater level of 141.81m (height 4.81m) and tailwater level of 138.81m (height 1.81m). On the upstream face, hydrostatic pressure and uplift were considered as usual. However, regarding the downstream face, only the effect of uplift pressure was considered, because in this case, hydrostatic pressure works as stabilizing load and was disregarded.

Materials properties are described in Table 1. The foundation block, where dam-foundation joints are resting, was considered rigid. To analyze the effect of sharing shear loads between foundation and anchor, we adopted different values for the anchor shear stiffness (50, 350, 550, 1000 and 2000 MN/m). These values reflect a range of parameters that could be inserted in St. John and Van Dillen (1983) and Lorig (1985) equations. For the friction angle of the rock-concrete contact interface we considered a wide range of possible values (30º, 37.5º, 45º, 52.5º and 60º).

Table 1. Properties of the materials

Parameter	
Concrete volumetric weight	24 kN/m^3
Water volumetric weight	10 kN/m^3
Rock-concrete (R-C) cohesion	null
R-C friction angle	various
R-C normal stiffness	10 GPa/m
R-C shear stiffness	3.33 GPa/m
Concrete Young's modulus	20 GPa
Concrete Poisson's ratio	0.2
Anchor Young's modulus	200 GPa
Anchor Poisson's ratio	0.29
Anchor axial stiffness	3000 MN/m
Anchor shear stiffness	various
Anchor axial ultimate capacity (tension)	400 MPa
Anchor shear ultimate capacity	168 kN

During the analysis an uplift update scheme was adopted in cracked zone along the base of the dam. In all cases, the final crack length corresponded to about 1 meter (approximately 29% of the total width), equivalent to an uplift pressure increase of about 16 kN, or approximately 13% of the initial uplift pressure. Total applied loads are shown in Table 2.

Table 2. Total request loads

Load description	[kN]
Dam self-weight	164.4
Downstream hydrostatic pressure	97.4
Uplift (initial condition)	120.8
Uplift (after crack)	136.7

4.2 *Effects of shear stiffness of the anchor*

Parametric analyses were made of the anchor shear stiffness for the values of 50, 350, 550, 1000 and 2000 MN/m, keeping constant the properties of the foundation plan, with a friction angle of 45° and null cohesion.

The results are shown in Table 3 and displacements observed in anchor and foundation in Table 4. The values of the shear forces in the anchor and along the foundation are shown in Figure 5. The tension that developed in the anchor is shown in Fig. 6, for the different shear stiffness values examined.

From these data it appears that the internal forces are not sensitive to anchor shear stiffness variation.

Table 3. Normal and shear forces in the anchor and in the concrete for different shear stiffnesses of the anchor (the concrete friction angle is constant, ϕ=45º) [kN]

$K_{s,a}$ [MN/m]	V_a	T_a	V_c	F_c
50	45.3	25.0	52.5	-52.7
350	44.8	25.0	53.0	-52.7
550	45.2	25.0	52.7	-52.7
1000	46.0	25.1	51.8	-52.8
2000	46.3	25.2	51.9	-52.9

Table 4. Normal and shear displacements in the anchor and in the concrete for different shear stiffnesses of the anchor (the concrete friction angle is constant, ϕ=45º) [x10^{-6} m]

$K_{s,a}$ [MN/m]	dV_a	dT_a	dV_c	dF_c
50	910.0	8.3	910.0	-2.6
350	130.0	8.3	130.0	-2.2
550	82.1	8.3	83.3	-2.6
1000	45.9	8.4	47.3	-2.6
2000	23.1	8.4	24.6	-2.7

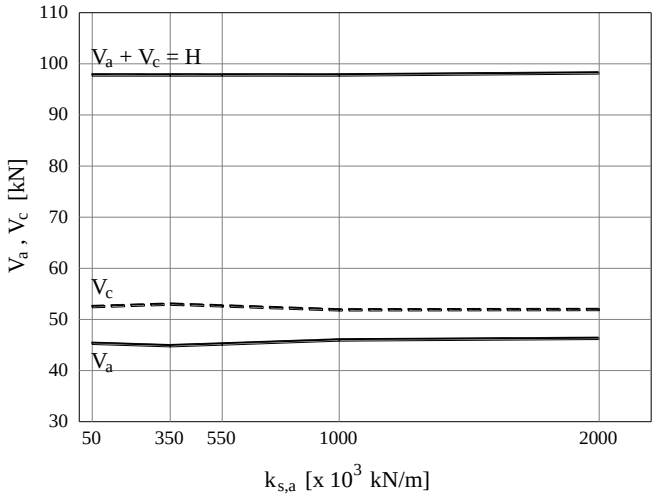

Figure 5 – Shear forces in the anchor and in the concrete for different shear stiffnesses of the anchor (the concrete friction angle is constant, ϕ=45º)

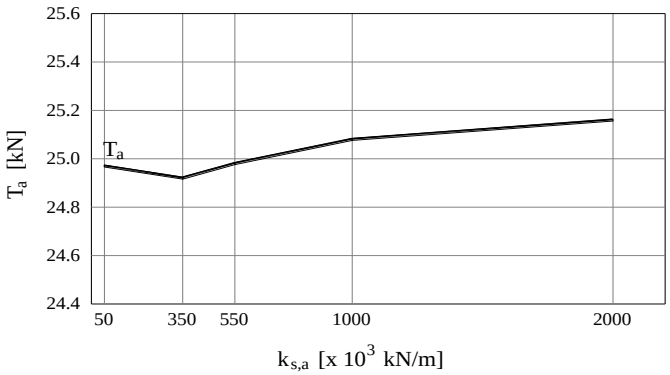

Figure 6 – Tensile force in the anchor for different shear stiffness of the anchor (the concrete friction angle is constant, ϕ=45º)

4.3 *Effect of friction angle at the rock-concrete interface*

Another parametric analysis was also made but now in relation to the friction angle (30º, 37.5º, 45º, 52.5º and 60º) of the rock-concrete interface for a null cohesion and constant anchor shear stiffness, equal to 1000 MN/m. The results are presented in Table 5 and displacements observed in Table 6.

Figure 7 represents the results of the shear forces in the anchor and in the foundation and Figure 7 the axial forces in the anchor.

Table 5. Normal and shear forces in the anchor and in the concrete for different concrete friction coefficients (angles) (the anchor shear stiffness is constant, $K_{s,a}$=1000 x MN/m) [kN]

ϕ	V_a	T_a	V_c	F_c
30 º	66.0	27.3	31.8	-55.0
37.5º	56.3	26.2	41.5	-54.0
45 º	46.0	25.1	51.8	-52.8
52.5º	33.0	23.6	64.8	-51.4
60 º	19.6	22.1	78.2	-49.9

Table 6. Normal and shear displacements in the anchor and in the concrete for different concrete friction coefficients (angles) (the anchor shear stiffness is constant, $K_{s,a}$=1000 MN/m) [x10^{-6} m]

ϕ	dV_a	dT_a	dV_c	dF_c
30 º	66.0	9.1	71.1	-3.0
37.5º	56.3	8.7	59.6	-2.8
45 º	45.9	8.4	47.3	-2.6
52.5º	32.9	7.9	31.8	-2.4
60 º	19.6	7.4	15.9	-2.1

In this case, that involves changes in the shear strength characteristics of the concrete-foundation interface, it is possible to observe an increase of

shear load split to the foundation, discharging the anchor as the friction angle is increased.

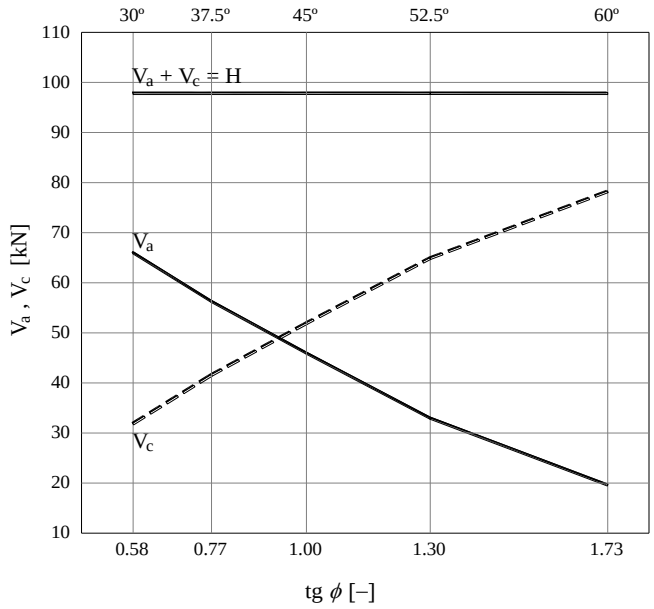

Figure 7 – Shear forces in the anchor and in the concrete for different concrete friction coefficients (angles) (the anchor shear stiffness is constant, Ks=1000 MN/m)

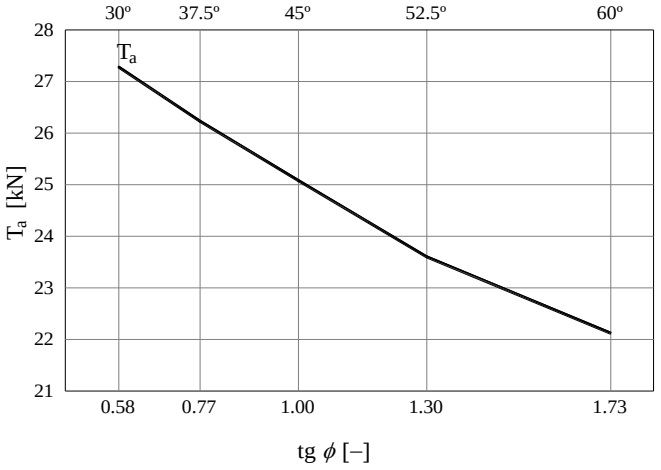

Figure 8 – Tensile force in the anchor for different concrete friction coefficients (angles) (the anchor shear stiffness is constant, Ks=1000 x103kN/m)

4.4 *Effect of multiple anchors*

A second anchor was included to original model (Fig. 9). The friction angle adopted for the rock-concrete interface was 45º, while anchor shear stiffness was 1000 MN/m, for both anchors. The remaining properties, as well as loads, match those already described. The final crack is similar to that observed in previous analysis, i.e. about 29% of the base was cracked. The results are presented in Table 7.

The comparison (Table 8) between 'one-anchor' and 'two-anchors' models shows an increase in the compressive stress on the concrete in the 'two-anchors' case, therefore concrete shear force is also larger. Thus the anchor shear force ($V_{a,1}$=46.0 kN) for the case 'one-anchor', is greater than the sum of the anchor shear forces ($V_{a,1}$+$V_{a,2}$=17.9+17.4 kN), for the case 'two-anchors'.

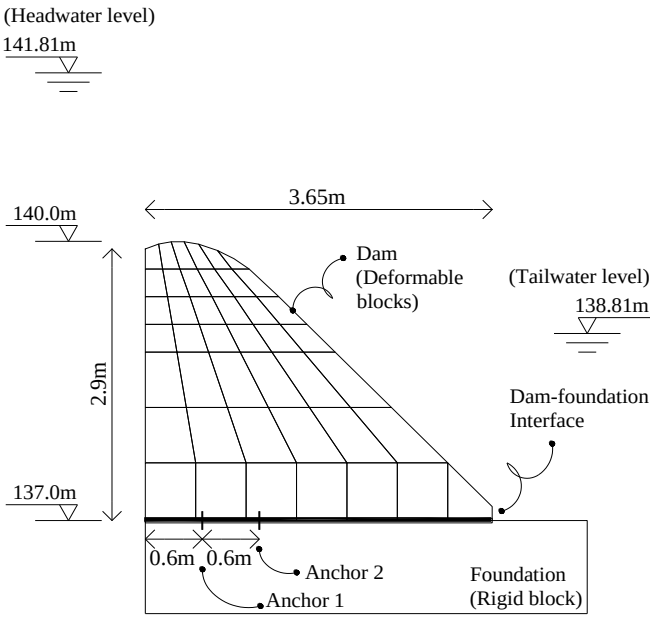

Figure 9. DEC-DAM 'two-anchors' model with geometry definition and load case

Table 7. Normal and shear forces in the anchor and in the concrete for (the anchor shear stiffness and the concrete friction angle are $K_{s,a}$=1000 MN/m and ϕ=45º, respectively)

Result	Force [kN]	Displ. [x10^{-6} m]
Axial force, Anchor 1 ($T_{a,1}$)	21.6	7.2
Shear force, Anchor 1 ($V_{a,1}$)	17.9	17.9
Axial force, Anchor 2 ($T_{a,2}$)	13.6	4.6
Shear force, Anchor 2 ($V_{a,2}$)	17.4	17.4
Axial force, Concrete (F_c)	-63.0	-2.75
Shear force, Concrete (V_c)	62.5	17.3

Table 8. Summary of results for models 'one-anchor' and 'two anchors' (the anchor shear stiffness and the concrete friction angle are $K_{s,a}$=1000 MN/m and ϕ=45º, respectively)

#Anchors	$T_{a,1}$	$T_{a,2}$	F_c	$V_{a,1}$	$V_{a,2}$	V_c
1	25.1	-	-52.8	46.0	-	51.8
2	21.6	13.6	-63.0	17.9	17.4	62.5

5 CONCLUSIONS

This paper presented the magnitude and distribution internal shear, tensile, compressive forces that develop in small gravity dams with passive steel anchor reinforcement. The distinct element method was used to obtain a solution that is in equilibrium, respect the compatibility of deformations and follow the material laws. It was found that:

(1) The shear stiffness of the anchor does not have a significant effect on the internal load magnitude and distribution.
(2) The computed displacements to mobilize the internal forces are extremely small (of the order of 10^{-5}m). This is a significant result because it is clearly shown that "large" displacements are not needed to develop significant loads.
(3) The dam-foundation friction angle is the most important parameter that will control the amount of shear load resisted by the anchor, while some variations in anchor tensile forces are noted.
(4) In the case of multiple anchors the effective lever arm of the anchors is reduced thus increasing the concrete normal force and related shear force resisted by the concrete.

ACKNOWLEDGMENTS

This work has been funded by FCT (Portuguese Foundation for Science and Technology) through the PhD grant SFRH/BD/43585/2008, for which the first author is grateful.

REFERENCES

3DEC, 2003, (3-Dimensionnal Distinct Element Code), User's Manual, Itasca Consulting Group Inc., Minnesota, USA.

Azuar, Debreuille, Habib, 1979, "Le renforcement des massifs rocheux par armatures passives" (Reinforcement of rock mass using passive anchors), Proceedings of the 4th ISMR Congress, Sept., Vol. 1, pp. 23-30.

Bjurstrom, S., 1974, "Shear Strength of Hard Rock Joints Reinforced by Grouted Untensioned Bolts", Proceedings of the 3rd International Congress on Rock Mechanics, Washington, D.C., National Academy of Sciences, Vol. II, Part B, pp. 1194-1199.

Bretas, E.M., Léger, P., Lemos, J.V., Lourenço, P.B, 2010a, "Avaliação de uma proposta de reforço de uma barragem gravidade" (Assessment of a reinforcement solution of a gravity dam), VII Simpósio sobre pequenas e médias centrais hidrelétricas, São Paulo, Brasil.

Bretas, E.M., Léger, P., Lemos, J.V., Lourenço, P.B, Ramos, J.M., 2010b, "Análise e reforço de barragens gravidade" (Analysis and reinforcement of gravity dams), Reabilitar 2010, Lisboa, Portugal.

Haas, C.J., 1976, "Shear Resistance of Rock Bolts", Transactions Society of Mining Engineering (AIME), Vol. 260, No. 1, pp. 32-41.

Lorig, L.J. 1985, "A Simple Numerical Representation of Fully Bonded Passive Rock Reinforcement for Hard Rocks", Computers and Geotechnics, Vol.1, pp. 79-97.

Pells, P.J.N., 1974, "The Behavior of Fully Bonded Rock Bolts", Proceedings of the 3rd International Congress on Rock Mechanics, Vol. 2, pp. 1212-1217.

St. John, C.M., Van Dillen, D.E., 1983, "Rock bolts: A new numerical representation and its application in tunnel design", 24th US Symposium on rock mechanics, Texas A. & M. University, USA, June, pp. 13-25.

UDEC, 2004, (Universal Distinct Element Code), User's Manual, Itasca Consulting Group Inc., Minnesota, USA.

USACE, 2005, "Stability Analysis of Concrete Structures", Report No. EM 1110-2-2100, December, US Corps of Engineers, Washington, D.C, USA.

Wyllie, D.C., 1999, "Foundation on Rock", 2nd Ed, E&FN Spon, London and New-York., 401 pp.